



## RESEARCH LETTER

10.1002/2015GL066873

## Key Points:

- Collocated space-based and ground-based data allow for near-cloud contamination to be removed
- Near-cloud contamination accounts for ~40% of the observed satellite-derived cloud lifetime effect
- The station-averaged and diurnally averaged net total aerosol direct + indirect radiative forcing is positive

## Supporting Information:

- Supporting Information S1
- Figure S1
- Figure S2
- Figure S3
- Figure S4
- Figure S5

## Correspondence to:

J. E. Ten Hoeve,  
john.tenhoever@noaa.gov

## Citation:

Ten Hoeve, J. E., and J. A. Augustine (2016), Aerosol effects on cloud cover as evidenced by ground-based and space-based observations at five rural sites in the United States, *Geophys. Res. Lett.*, *43*, 793–801, doi:10.1002/2015GL066873.

Received 5 NOV 2015

Accepted 24 NOV 2015

Accepted article online 1 DEC 2015

Published online 19 JAN 2016

Published 2015. This article is a U.S. Government work and is in the public domain in the USA.

## Aerosol effects on cloud cover as evidenced by ground-based and space-based observations at five rural sites in the United States

John E. Ten Hoeve<sup>1</sup> and John A. Augustine<sup>2</sup>

<sup>1</sup>National Weather Service, Silver Spring, Maryland, USA, <sup>2</sup>Global Monitoring Division, Earth Systems Research Laboratory, Boulder, Colorado, USA

**Abstract** Previous studies of the second aerosol indirect (lifetime) effect on cloud cover have estimated the strength of the effect without correcting for near-cloud contamination and other confounding factors. Here we combine satellite-based observations with a multiyear ground-based data set across five rural locations in the United States to more accurately constrain the second indirect aerosol effect and quantify aerosol effects on radiative forcing. Results show that near-cloud contamination accounts for approximately 40% of the satellite-derived aerosol-cloud relationship. When contamination is removed and the effect of meteorological covariation is minimized, a strong physical aerosol effect on cloud cover remains. Averaged over all stations and after correcting for contamination, the daytime solar and total (solar + IR) radiative forcing is  $-52 \text{ W/m}^2$  and  $-19 \text{ W/m}^2$ , respectively, due to both direct and indirect aerosol effects for aerosol optical depths ( $\tau$ ) between 0 and 0.3. Averaged diurnally, the average total radiative forcing is  $+16 \text{ W/m}^2$ .

### 1. Introduction

The effect of aerosols on cloud cover (i.e., cloud lifetime effect) remains one of the largest uncertainties in the climate system [Stocker et al., 2013]. With the advent of satellite remote sensing, our ability to detect microphysical and dynamical aerosol effects on the macroscopic properties of clouds has greatly improved [Kaufman et al., 2005a; Koren et al., 2005; Yuan et al., 2011]. In particular, several satellite-based studies have documented the effect of aerosols on the thickness and horizontal extent of ship tracks [Ackerman et al., 1995; Christensen and Stephens, 2011]. Aerosol effects on clouds have been studied using models of varying length and time scales [Fan et al., 2013; Myhre et al., 2007; Quaas et al., 2010], yet many global models still do not accurately reproduce observed relationships [Quaas et al., 2009]. Due to the complex interaction between microphysical and dynamical effects and the fact that neither satellite observations nor global models can directly observe nor resolve the microphysical processes that contribute to the aerosol optical depth ( $\tau$ )-cloud fraction ( $f_c$ ) relationship, the cloud lifetime effect remains an area of active study.

Many observational and modeling studies have found a strong increase in  $f_c$  with increasing  $\tau$ , particularly at  $\tau < 0.3$  [e.g., Myhre et al., 2007]. Yet some studies indicate a reduction in  $f_c$  for shallow cumulus clouds, particularly in regions with absorbing aerosol and at  $\tau > 0.2$ – $0.3$  [Koren et al., 2008; Ten Hoeve et al., 2012]. While some studies attribute the increase in  $f_c$  to aerosol microphysical effects, a portion of the positive  $\tau$ - $f_c$  correlation has been hypothesized to result from confounding factors including 3-D scattering of radiation off cloud sides [Varnai and Marshak, 2009], aerosol humidification near clouds [Twohy et al., 2009], cloud contamination of the aerosol retrieval and vice versa [Kaufman et al., 2005b], vertical overlap of aerosols and clouds [Devasthale and Thomas, 2011], and meteorological covariation [Engstrom and Ekman, 2010; Grandey et al., 2013; Mauger and Norris, 2007]. Observational satellite-based studies have attempted to account for these confounding factors through a variety of methods, but it remains difficult to completely remove all of these factors and target only physical aerosol-cloud effects using satellite-based sensors alone [Grandey et al., 2013; Gryspeerd et al., 2014; Jeong and Li, 2010; Koren et al., 2010; Loeb and Schuster, 2008].

Studies have employed ground-based Atmospheric Radiation Measurement (ARM) site measurements to explore aerosol-cloud interactions [Jeong and Li, 2010; Li et al., 2011; Zhao et al., 2012; Yan et al., 2014]. Some of these studies focused on a localized region, such as the Southern Great Plains (SGP) of the U.S. and the first indirect effect rather than the cloud lifetime effect [Li et al., 2011; Zhao et al., 2012]. Niu and Li [2012] supported

the findings of *Li et al.* [2011] over the tropics using an ensemble of satellite data. *Jeong and Li* [2010] used ground-based SGP ARM data to study the cloud lifetime effect and found a positive relationship between cloud fraction and aerosol optical thickness after accounting for confounding factors such as aerosol humidification and cloud contamination of the aerosol retrieval and vice versa.

This study builds on previous studies by combining traditional satellite data sets from the Moderate Resolution Imaging Spectroradiometer (MODIS) with a long-running, geographically distributed, and climatically diverse ground-based data set never before used for this purpose from the U.S. Surface Radiation Budget Network (SURFRAD) [Augustine et al., 2000] to analyze  $\tau$ - $f_c$  relationships and their impact on surface radiative forcing. The advantage of using ground station data is that collocated radiation, aerosol, meteorological, and cloud coverage measurements allow many of the aforementioned confounding factors to be more effectively removed compared to satellite-based methods alone, thus better isolating the true physical relationship between aerosols and cloud cover.

## 2. Methods

The National Oceanic and Atmospheric Administration (NOAA) administers the SURFRAD network to support climate research with accurate, continuous, long-term measurements of the surface radiation budget over the United States. One minute averages of 1 s samples have been made since 1 January 2009, whereas 3 min averages have been reported from 1995 through 2008. The network currently operates seven stations in remote locations of the United States. The five SURFRAD stations used in this study are shown in Figure S1 in the supporting information. The station at Desert Rock, NV is not included due to infrequent cloud cover and the station at Sioux Falls, SD is not included due to excessive missing  $f_c$  data over the core study period. This study encompasses the period from 2006 to 2011, except for Penn State, PA, which is restricted to 2006 to 2009 due to missing  $\tau$  data after 2009.

For this analysis,  $\tau$ ,  $f_c$ , and radiation data from the five SURFRAD stations are averaged over 1 h periods and compared to collocated MODIS aerosol and cloud retrievals [Platnick et al., 2003; Remer et al., 2005]. SURFRAD stations have a higher temporal resolution than sun-synchronous satellites with periodic overpasses, but a significantly smaller spatial resolution. Yet ground-based observations have unique benefits over space-based sensors, such as the ability to detect diurnal cycles and to account for the transition zone between cloud-contaminated and unobstructed observations by sampling before and after a cloud passes. Since SURFRAD and MODIS require the sun to be unobstructed to observe  $\tau$ , observations of overcast or nearly overcast scenes are not included, restricting the analysis to clear, scattered, or broken skies.

Aerosol optical depth ( $\tau$ ) retrievals are made for SURFRAD sites using data from a visible MultiFilter Rotating Shadowband Radiometer (MFRSR) [Harrison et al., 1994]. The MFRSR is a Sun photometer that infers the solar beam intensity by computing the difference between successive global and diffuse measurements.  $\tau$  is computed at nominal wavelengths of 415, 500, 614, 670, and 870 nm using the Beer-Lambert equation and accounting for Rayleigh scattering and ozone absorption [Augustine et al., 2008]. The Ångström exponent (AE), calculated using the 500 nm and 614 nm channel pair, is used to estimate  $\tau$  at 550 nm to match the MODIS retrieval. The aerosol index, defined as the product of the  $\tau$  and the AE, is sometimes used as a proxy for cloud condensation nuclei. However, since the MODIS AE retrieval over land is often unreliable, we elect to use  $\tau$  as the proxy in this study [Levy et al., 2010]. Cloud screening is performed using the intersection of two stability algorithms that test inhomogeneity in the  $\tau$  time series [Augustine et al., 2008]. Good comparisons with collocated high-quality AERONET sites validate the MFRSR retrieval and the hybrid cloud screening method.

Cloud cover data are retrieved at the SURFRAD stations using a Total Sky Imager (TSI) [Long et al., 2006]. The TSI consists of a web camera suspended over a convex mirror. Images of the sky are collected and automatically processed into 160° field of view (FOV)  $f_c$  data at a 1 min frequency. Studies have indicated good comparisons between TSI data and meteorological observers [Huo and Lu, 2012]. However, the results of *Kassianov et al.* [2005] show that restricting the TSI image to the zenith  $\pm 50^\circ$  (100° FOV) best approximates the nadir-projected  $f_c$  of a satellite view by eliminating cloud overlap and cloud side-view errors in the outer band of the full 160° FOV TSI image, which artificially increase  $f_c$ . For broken cloud fields, the domain-averaged nadir-projected cloud fraction estimated by a 100° FOV is roughly 10% less than from the 160° FOV TSI image [Kassianov et al., 2005]. Since our study uses clear or broken cloud fields to observe aerosols

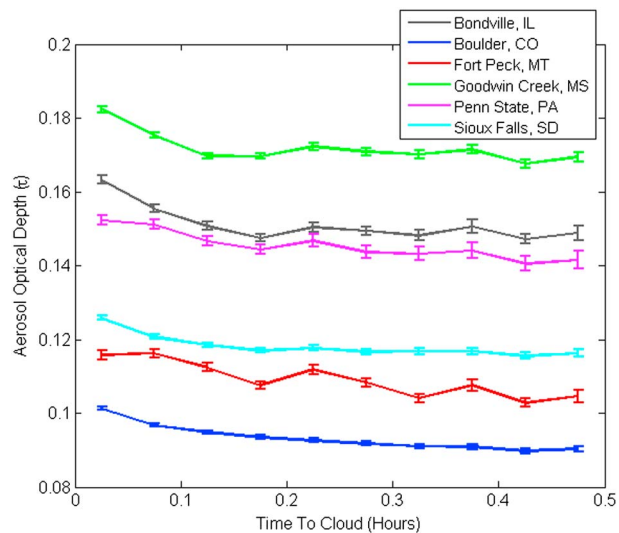


**Figure 1.**  $\tau$  at 550 nm binned by time to the nearest cloud for observations over all years and all daytime hours for each SURFRAD station.  $\tau$  is higher for times under  $\sim 0.3$  h, suggesting aerosol humidification or brightening may artificially increase MFRSR  $\tau$  retrievals near clouds.

downwelling (upwelling) solar and thermal infrared radiation are measured by an upward facing (downward facing) pyranometer and pyrgeometer, respectively. The upward facing pyranometer's global solar measurement is considered secondary to the sum of the direct and diffuse solar measurements, which is a more accurate representation of downwelling solar and is also available at SURFRAD stations. Net solar calculations reported in SURFRAD data files are computed using the direct and diffuse measurements, when available, for the downwelling solar component.

### 3. Results

Sun photometer measurements are sensitive to the transition zone near cloud edges. In addition to sensing swelled aerosols near clouds,  $\tau$  can be enhanced by 3-D effects near clouds because the MFRSR uses inferred direct (computed as the difference between successive cosine-corrected global and diffuse measurements) to determine  $\tau$ . Side-scattered photons intercepting the MFRSR could disproportionately increase the diffuse measurement, thus artificially enhancing  $\tau$ . To correctly assess the effect of aerosol on  $f_c$ , it is imperative that near-cloud aerosol retrievals are removed to avoid spurious  $\tau$ - $f_c$  correlations. Figure 1 shows  $\tau$  for each station as a function of time from a cloud-contaminated retrieval, as determined by the cloud screening algorithm. Because the actual distance from the cloud depends on the wind speed, the time-to-cloud measurement serves as a proxy for the distance away from the cloud, which is the actual variable of interest. Composite results for all stations and all times in Figure 1 show that near a cloud,  $\tau$  is elevated on average by 6–11% depending on the location, due to near-cloud confounding effects, compared to periods greater than  $\sim 0.3$  h from the cloud when  $\tau$  appears to be nearly constant. The magnitude of this fractional increase in  $\tau$  near clouds is consistent with previous studies [Altaratz *et al.*, 2013; Bar-Or *et al.*, 2012]. This suggests that aerosol humidification and/or brightening may artificially increase MFRSR  $\tau$  retrievals near clouds.

In Figure 2, hourly-averaged  $f_c$  is binned by hourly averaged  $\tau$  for each SURFRAD station and composited across all stations for retrievals within 1.5 h of the  $\sim 1:30$  P.M. overpass time of the Aqua satellite. To elucidate the impact of near-cloud confounding effects,  $\tau$  is averaged over 1 h periods using two approaches, first using all values of  $\tau$  (referred to as uncorrected) and then to remove near-cloud confounding effects in the aerosol retrievals using only values of  $\tau$  where the time-to-cloud measurement exceeds 0.3 h (referred to as corrected). Since the TSI has been shown to misinterpret heavy aerosol for thin cloud, only opaque clouds, as defined by the TSI algorithm are retained. The threshold between thin and opaque clouds is determined for each TSI by comparing the red-to-blue ratio of the TSI camera in the processed image to human observations.

and clouds together, SURFRAD 160° FOV TSI-based mean cloud fractions are reduced by 10% to better compare to the nadir view cloud fractions of MODIS.

MODIS Aqua Collection 5.1 Level 2 retrievals over an approximate 30 km  $\times$  30 km footprint centered on each SURFRAD station from 2008 and 2009 are used as complete SURFRAD data were available for those years. The footprint approximately matches the viewing area of the SURFRAD TSI and ensures a large enough sample size. MODIS Level 2, 5 km  $\times$  5 km  $f_c$  is calculated for each 10 km  $\times$  10 km  $\tau$  pixel as in Ten Hoeve *et al.* [2011].

Aerosol direct and indirect radiative forcing (RF) are quantified for each SURFRAD station. At SURFRAD stations,

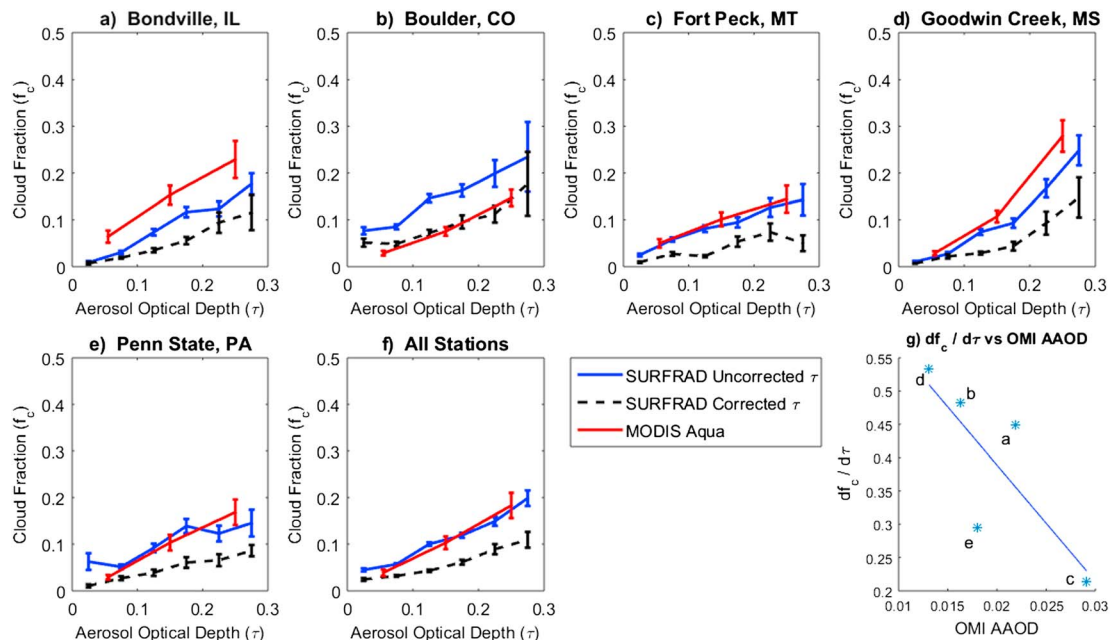


**Figure 2.** (a–e) Hourly-averaged  $f_c$  binned by  $\tau$  for the five SURFRAD stations and (f) data integrated over all stations, collocated in time and space with MODIS Aqua retrievals. Results using all  $\tau$  observations (blue line—uncorrected  $\tau$ ) and results using only  $\tau$  observations where the time-to-cloud measurement is greater than 0.3 h (dashed black line—corrected  $\tau$ ) discriminate between results with near-cloud contamination not removed and removed, respectively. Red lines show the relationships derived from collocated MODIS Level 2 Aqua retrievals. For Figure 2f, the uncorrected  $\tau$  relationship is based on a total of 6125 observations, the corrected  $\tau$  relationship is based on 4169 observations, and the MODIS Aqua relationship is based on 3003 observations. (g)  $df_c/d\tau$  versus OMI-derived AAOD; point labels within refer to SURFRAD stations corresponding to Figures 2a–2e).

Figure 2 is restricted to  $\tau < 0.3$  since previous studies show microphysical aerosol-cloud effects saturate at  $\tau > 0.3$  and heavy aerosol may be misinterpreted as cloud [Brennan *et al.*, 2005; Small *et al.*, 2011; Koren *et al.*, 2014]. Further, over 96% of SURFRAD  $\tau$  observations occur at  $\tau < 0.3$  (Table S1); therefore, our analysis already includes most  $\tau$  observations. By comparing  $\tau$ - $f_c$  data derived from MODIS to the corrected and uncorrected SURFRAD data, the influence of near-cloud contamination on the satellite-derived second aerosol indirect effect can be studied and the value of MODIS to these types of studies ascertained.

A positive  $\tau$ - $f_c$  relationship is observed at all stations for both the uncorrected and corrected  $\tau$  relationships. For four of the five geographically distributed stations, MODIS  $\tau$ - $f_c$  relationships match the uncorrected SURFRAD  $\tau$ - $f_c$  relationship better than the corrected  $\tau$ - $f_c$  relationship, and in the majority of those stations, the standard errors of uncorrected SURFRAD and MODIS relationships overlap at points, indicating no significant difference between the uncorrected SURFRAD relationships and those of MODIS.

Figure 2f shows the all-station composite result.  $df_c/d\tau$  of the corrected  $\tau$  relationship is 58% of the uncorrected  $\tau$  relationship ( $df_c/d\tau$  of 0.35 versus 0.61), suggesting that near-cloud contamination accounts for ~40% of the  $df_c/d\tau$  relationship. Further, the all-station MODIS result is nearly identical to the composite SURFRAD uncorrected  $\tau$ - $f_c$  relationship. The different  $df_c/d\tau$  slopes between the corrected and uncorrected relationships, and the similarity of the MODIS result to the uncorrected SURFRAD results, strongly suggest that near-cloud contamination may be present to some extent in the MODIS observations, artificially enhancing the effect of aerosols on cloud cover in MODIS-based studies. Further, the positive  $df_c/d\tau$  slope of the corrected  $\tau$  result in Figure 2f indicates that confounding effects cannot explain the entire relationship and that physical aerosol-cloud effects are likely to play a substantial role at low to moderate  $\tau$ .

$df_c/d\tau$  of the corrected  $\tau$  relationships varies by location, ranging between 0.21 for Fort Peck and 0.53 for Goodwin Creek. While these differences may be influenced by numerous microphysical and dynamical factors, aerosol composition has been hypothesized to play a substantial role. We use Level 3 OMAEROe aerosol absorption optical depth (AAOD) retrievals at 483.5 nm from the Ozone Monitoring Instrument (OMI), averaged over 2006–2011 and over each SURFRAD station, as a proxy for aerosol composition [Torres *et al.*, 2007]. We then regress  $df_c/d\tau$  against the AAOD retrievals. Results in Figure 2g indicate a prominent negative relationship

between AOD and  $df_c/d\tau$ , suggesting that the greater the aerosol absorption, the greater the tempering of the aerosol indirect effect due to the offsetting semidirect effect. It is important to note that these correlations do not imply causation, and other factors may play a role. However, these findings do suggest that aerosol composition may be one of the primary contributors to the variation in observed aerosol-cloud indirect effects across SURFRAD locations.

The influence of meteorology on the relationships in Figure 2 cannot be ignored. Meteorological variables, including surface wind speed (WSPD), relative humidity (RH), and sea level pressure (SLP), have been shown to influence both  $\tau$  and  $f_c$  together, resulting in a  $\tau$ - $f_c$  relationship dominated not by aerosol indirect effects but instead by meteorological covariation [Engstrom and Ekman, 2010; Mauger and Norris, 2007]. However, the fact that all of the geographically dispersed SURFRAD stations, with different meteorological regimes, present similar  $\tau$ - $f_c$  relationships suggests that meteorology is likely not the dominant driver of the relationships in Figure 2. The use of a long multiyear data set at each station further suppresses the impact of meteorology on the observed relationships. Yet, to investigate the effect of meteorology on the results, we identify possible meteorological variables that could influence the observed relationships using the methodology in Koren *et al.* [2010] and assess their influence through data stratification.

We employ hourly-averaged meteorological measurements from SURFRAD stations to determine any correlation with corrected hourly  $\tau$  and  $f_c$ . Figure S2 indicates that RH and SLP are positively and negatively correlated, respectively, with both  $\tau$  and  $f_c$ , and thus could contribute to the positive  $\tau$ - $f_c$  relationships in Figure 2. Temperature (Temp) and WSPD are not correlated with  $\tau$  and  $f_c$  in the same direction for most stations, and so these meteorological variables are unlikely to influence the positive  $\tau$ - $f_c$  relationships. We account for the variation of RH and SLP by slicing the SURFRAD retrievals into bins of similar meteorology. Figure S3 shows RH and SLP binned by  $\tau$  for multiple slices of RH and SLP for each SURFRAD station. RH and SLP do not greatly vary with  $\tau$  within each bin and therefore should not be a strong driver of the  $\tau$ - $f_c$  relationships. Figure 3 shows  $f_c$  binned by corrected  $\tau$  for the same stratifications of RH and SLP in Figure S3. Figure 3 shows that  $df_c/d\tau$  is positive and of a similar slope to the corrected  $\tau$  relationships in Figure 2 across all SURFRAD stations and nearly all slices. We perform similar analyses with 850 hPa RH and lower tropospheric stability in Figure S4 and also find positive values of  $df_c/d\tau$  across slices of these variables. While this analysis suggests that meteorology does not significantly influence the  $\tau$ - $f_c$  relationships, we cannot rule out other meteorological variables, not accounted for here, which may have a greater influence. Yet, these results are consistent with other studies that indicate meteorological covariation does not dominate observed  $\tau$ - $f_c$  relationships and that microphysical and macrophysical aerosol effects likely play a substantial role.

A benefit of collocated surface radiation budget and  $\tau$  measurements at SURFRAD stations is the capability to directly measure the impact of aerosol effects on the local surface radiative forcing. Figure S5 shows that instantaneous net solar (IR) radiation consistently decreases (increases) with increasing corrected  $\tau$  for different slices of solar zenith angle (SZA) and for all stations. This result represents the total aerosol effect, which includes both the direct effect and the first and second indirect effects.

Rows 1–7 of Table 1 show combined aerosol direct and indirect instantaneous radiative forcing (RF) of solar, IR, and total (solar + IR) net radiation for  $\tau$  between 0 and 0.3, averaged over all SURFRAD stations, and for various slices of SZA. The RF is calculated by fitting a linear trend line to each  $\tau$ -radiation relationship and calculating the change between  $\tau$  values of 0 and 0.3. Results indicate that solar and solar + IR RFs are relatively similar across all SZAs, except for  $SZA < 25^\circ$  where they are more negative due to strong solar insolation at high Sun, and for  $SZA > 75^\circ$  where they are less negative, or slightly positive, due to the reduction in solar insolation at low Sun, even considering the greater fraction of upscattered radiation at large SZAs [Nemesure *et al.*, 1995; Zhou, 2006]. Consistent with previous studies [e.g., Yan *et al.*, 2014], IR RF is positive and similar across all SZAs.

Rows 8–13 of Table 1 show aerosol RF averaged over SZAs between  $15^\circ$  and  $85^\circ$  by station and averaged over all stations. Equations (3)–(6) in Yan *et al.* [2014] are used to average across SZAs. Results show that SURFRAD stations with larger  $df_c/d\tau$  slopes, such as Goodwin Creek, Boulder, and Bondville, exhibit larger solar and IR aerosol RFs, whereas stations with smaller  $df_c/d\tau$  slopes exhibit smaller solar and IR RFs, as expected. The network composite daytime average solar and IR RFs are  $-52$  and  $+33$   $W/m^2$ , respectively. Yet because solar and IR RFs vary together, the total solar + IR RF is similar across all stations, with an average of  $-19$   $W/m^2$ . These

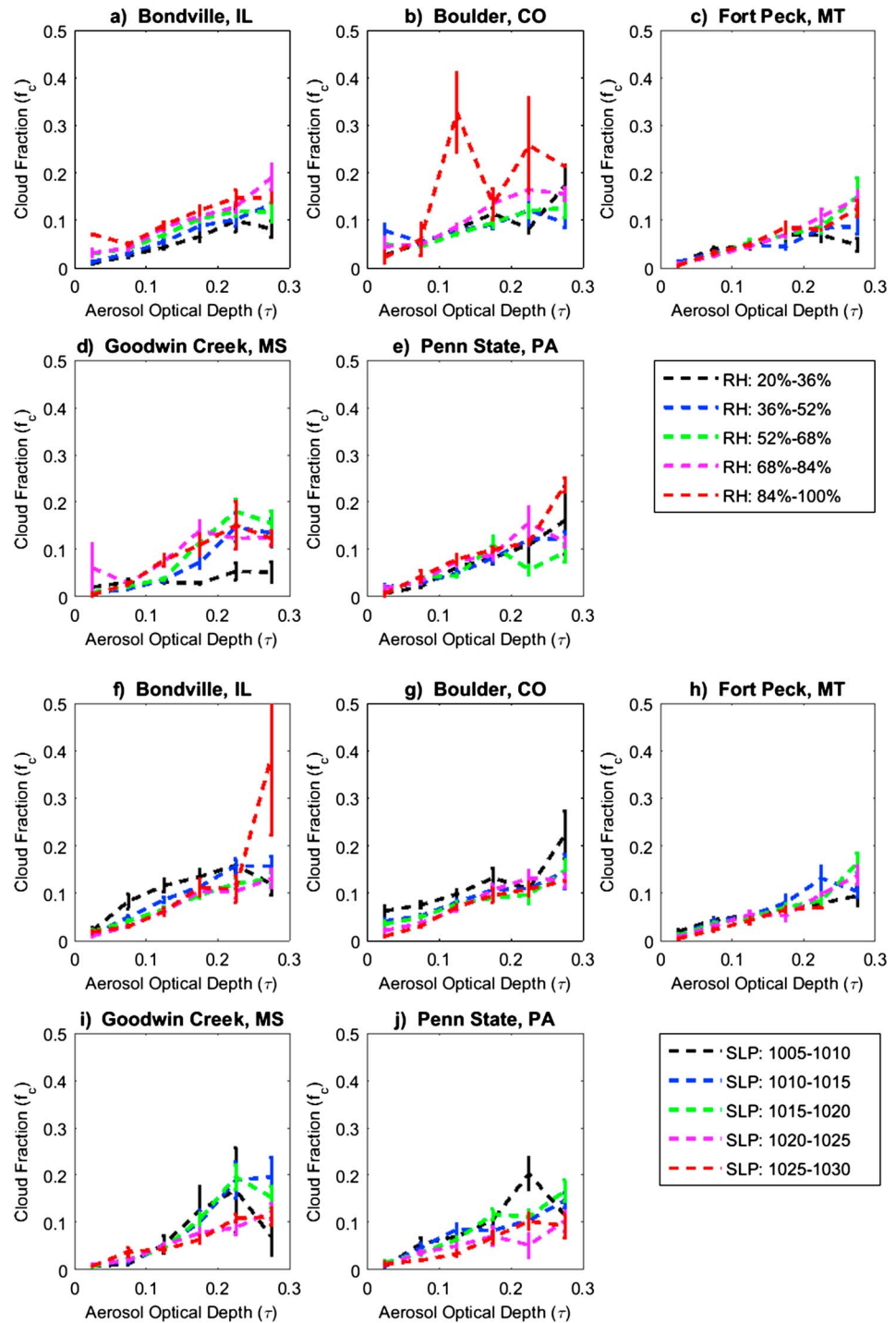


**Figure 3.** Hourly-averaged  $f_c$  binned by  $\tau$  corrected for near-cloud contamination for different slices of (a–e) relative humidity (RH) and (f–j) sea level pressure (SLP) for the five SUFRAD stations. In Figure 3g, slices for Boulder, CO are 30 hPa less than the other stations.

daytime RF results are consistent with a satellite-based study over the pristine ocean and a ground-based study over a limited area in the SGP [Koren et al., 2014; Yan et al., 2014].

Since the MFRSR cannot measure  $\tau$  at night, it is impossible to directly calculate diurnally averaged aerosol RF estimates. However, because IR RF is relatively constant across all SZAs during the daytime for each station,

**Table 1.** Rows 1–7: Net Solar, Net IR, and Net Total (Solar + IR) Aerosol Radiative Forcing (RF) ( $\text{W/m}^2$ ) Including Direct and Indirect Aerosol Effects, for  $\tau$  Between 0 and 0.3 Corrected for Near-Cloud Contamination, Averaged Over All SURFRAD Stations, and for Various Bins of SZA; Rows 8–13: Daytime Aerosol RF ( $\text{W/m}^2$ ) Averaged Over SZAs Between  $15^\circ$  and  $85^\circ$  for Each SURFRAD Station and Averaged Over All Stations

Row #	Solar Zenith Angle	Net Solar Radiative Forcing ( $\text{W/m}^2$ )	Net IR Radiative Forcing ( $\text{W/m}^2$ )	Net Total Solar + IR Radiative Forcing ( $\text{W/m}^2$ )
1	$15^\circ$ – $25^\circ$	–74	+42	–32
2	$25^\circ$ – $35^\circ$	–62	+42	–20
3	$35^\circ$ – $45^\circ$	–45	+37	–9
4	$45^\circ$ – $55^\circ$	–62	+34	–28
5	$55^\circ$ – $65^\circ$	–55	+30	–25
6	$65^\circ$ – $75^\circ$	–58	+29	–28
7	$75^\circ$ – $85^\circ$	–18	+22	+5
8	Bondville, IL	–51	+36	–15
9	Boulder, CO	–51	+20	–31
10	Fort Peck, MT	–32	+5	–27
11	Goodwin Creek, MS	–84	+68	–16
12	Penn State, PA	–44	+37	–7
13	All Station Daytime Average	–52	+33	–19

diurnally averaged IR RF may be estimated by assuming that the daytime average applies at night. Using zero solar RF at night and our measured values during the daytime, the diurnally averaged network composite total aerosol RF (solar + IR) is  $+16 \text{ W/m}^2$ , suggesting that overall, aerosol direct and indirect effects result in net warming at the surface. These results indicate that combined aerosol direct and indirect effects have a substantial impact on the local energy balance at these five SURFRAD stations.

#### 4. Conclusions

This study employs the long-running and geographically dispersed ground-based SURFRAD data set to study aerosol effects on cloud cover and surface radiative forcing over the rural United States. Aerosol retrievals near clouds are removed to minimize confounding factors such as 3-D scattering effects and aerosol humidification and to compare relationships between cloud fraction ( $f_c$ ) and aerosol optical depth ( $\tau$ ) to similar relationships retrieved from MODIS. For most stations, MODIS  $\tau$ - $f_c$  relationships match the uncorrected SURFRAD  $\tau$ - $f_c$  relationships where near-cloud contamination is not removed, suggesting confounding factors affect the satellite-derived relationships. Yet even when near-cloud contamination is removed from the SURFRAD data, we still find that  $f_c$  increases with increasing  $\tau$ , suggesting that a physical response of cloud fraction to increasing aerosol loading occurs. Specifically, we find that near-cloud contamination accounts for roughly 40% of the uncorrected satellite-derived  $df_c/d\tau$  relationship, which is consistent with a previous study that estimated the contamination using satellite observations alone [Gryspeerd *et al.*, 2014]. These results are also consistent with Jeong and Li [2010] over the SGP where a minority of the observed  $\tau$ - $f_c$  relationship was attributed to confounding factors such as aerosol humidification. Our study also suggests that differences in  $df_c/d\tau$  across SURFRAD stations may be attributed to differences in aerosol composition.

The effect of meteorological covariation on  $\tau$ - $f_c$  relationships is also investigated. Surface air temperature, wind speed, atmospheric pressure, surface and 850 hPa relative humidity, and lower tropospheric stability do not appreciably influence  $\tau$ - $f_c$  relationships; however, we cannot rule out other meteorological parameters we have not tested.

Utilizing SURFRAD radiation measurements, we find that the net RF due to combined direct and indirect aerosol effects, averaged over all stations and daytime SZAs, is  $-52 \text{ W/m}^2$  and  $+33 \text{ W/m}^2$  for solar and IR, respectively, resulting in a net total daytime solar + IR RF of  $-19 \text{ W/m}^2$ . However, averaged diurnally, the net total solar + IR RF is  $+16 \text{ W/m}^2$ . Our results indicate that aerosols have a substantial impact on the surface energy balance and that before making assessments of aerosol-cloud interactions it is critical that  $\tau$  measurements be corrected for near-cloud contamination.

### Acknowledgments

We thank Tom Eck, Jens Redemann, Lorraine Remer, and Chuck Long for providing helpful comments on this work. MODIS data are available at <http://ladsweb.nascom.nasa.gov/>, and SURFRAD data are available at <http://www.esrl.noaa.gov/gmd/grad/surfrad/>.

### References

- Ackerman, A. S., O. B. Toon, and P. V. Hobbs (1995), Numerical modeling of ship tracks produced by injections of cloud condensation nuclei into marine stratiform clouds, *J. Geophys. Res.*, *100*(D4), 7121–7133, doi:10.1029/95JD00026.
- Altaratz, O., R. Z. Bar-Or, U. Wollner, and I. Koren (2013), Relative humidity and its effect on aerosol optical depth in the vicinity of convective clouds, *Environ. Res. Lett.*, *8*(3), doi:10.1088/1748-9326/8/3/034025.
- Augustine, J. A., J. J. DeLuise, and C. N. Long (2000), SURFRAD—A national surface radiation budget network for atmospheric research, *Bull. Am. Meteorol. Soc.*, *81*(10), 2341–2357.
- Augustine, J. A., G. B. Hodges, E. G. Dutton, J. J. Michalsky, and C. R. Cornwall (2008), An aerosol optical depth climatology for NOAA's national surface radiation budget network (SURFRAD), *J. Geophys. Res.*, *113*, D11204, doi:10.1029/2007JD009504.
- Bar-Or, R. Z., I. Koren, O. Altaratz, and E. Fredj (2012), Radiative properties of humidified aerosols in cloudy environment, *Atmos. Res.*, *118*, 280–294.
- Brennan, J. I., Y. J. Kaufman, I. Koren, and R. R. Li (2005), Aerosol-cloud interaction-misclassification of MODIS clouds in heavy aerosol, *IEEE Trans. Geosci. Remote Sens.*, *43*(4), 911–915.
- Christensen, M. W., and G. L. Stephens (2011), Microphysical and macrophysical responses of marine stratocumulus polluted by underlying ships: Evidence of cloud deepening, *J. Geophys. Res.*, *116*, D03201, doi:10.1029/2010JD014638.
- Devasthale, A., and M. A. Thomas (2011), A global survey of aerosol-liquid water cloud overlap based on four years of CALIPSO-CALIPSO data, *Atmos. Chem. Phys.*, *11*(3), 1143–1154.
- Engstrom, A., and A. M. L. Ekman (2010), Impact of meteorological factors on the correlation between aerosol optical depth and cloud fraction, *Geophys. Res. Lett.*, *37*, L18814, doi:10.1029/2010GL044361.
- Fan, J., L. R. Leung, D. Rosenfeld, Q. Chen, Z. Li, J. Zhang, and H. Yan (2013), Microphysical effects determine macrophysical response for aerosol impacts on deep convective clouds, *Proc. Nat. Acad. Sci. U.S.A.*, *110*(48), E4581–E4590.
- Grandey, B. S., P. Stier, and T. M. Wagner (2013), Investigating relationships between aerosol optical depth and cloud fraction using satellite, aerosol reanalysis and general circulation model data, *Atmos. Chem. Phys.*, *13*(6), 3177–3184.
- Gryspeerd, E., P. Stier, and D. G. Partridge (2014), Satellite observations of cloud regime development: the role of aerosol processes, *Atmos. Chem. Phys.*, *14*(3), 1141–1158.
- Harrison, L., J. Michalsky, and J. Berndt (1994), Automated multifilter rotating shadow-band radiometer—An instrument for optical depth and radiation measurements, *Appl. Opt.*, *33*(22), 5118–5125.
- Huo, J., and D. Lu (2012), Comparison of cloud cover from all-sky imager and meteorological observer, *J. Atmos. Oceanic Technol.*, *29*(8), 1093–1101.
- Jeong, M.-J., and Z. Li (2010), Separating real and apparent effects of cloud, humidity, and dynamics on aerosol optical thickness near cloud edges, *J. Geophys. Res.*, *115*, D00K32, doi:10.1029/2009JD013547.
- Kassianov, E., C. N. Long, and M. Ovtchinnikov (2005), Cloud sky cover versus cloud fraction: Whole-sky simulations and observations, *J. Appl. Meteorol.*, *44*, 86–98.
- Kaufman, Y. J., I. Koren, L. A. Remer, D. Rosenfeld, and Y. Rudich (2005a), The effect of smoke, dust, and pollution aerosol on shallow cloud development over the Atlantic Ocean, *Proc. Nat. Acad. Sci. U.S.A.*, *102*(32), 11,207–11,212.
- Kaufman, Y. J., et al. (2005b), A critical examination of the residual cloud contamination and diurnal sampling effects on MODIS estimates of aerosol over ocean, *IEEE Trans. Geosci. Remote Sens.*, *43*(12), 2886–2897.
- Koren, I., Y. J. Kaufman, D. Rosenfeld, L. A. Remer, and Y. Rudich (2005), Aerosol invigoration and restructuring of Atlantic convective clouds, *Geophys. Res. Lett.*, *32*, L14828, doi:10.1029/2005GL023187.
- Koren, I., J. V. Martins, L. A. Remer, and H. Afargan (2008), Smoke invigoration versus inhibition of clouds over the Amazon, *Science*, *321*(5891), 946–949.
- Koren, I., G. Feingold, and L. A. Remer (2010), The invigoration of deep convective clouds over the Atlantic: Aerosol effect, meteorology or retrieval artifact?, *Atmos. Chem. Phys.*, *10*(18), 8855–8872.
- Koren, I., G. Dagan, and O. Altaratz (2014), From aerosol-limited to invigoration of warm convective clouds, *Science*, *344*(6188), 1143–1146.
- Levy, R. C., L. A. Remer, R. G. Kleidman, S. Mattoo, C. Ichoku, R. Kahn, and T. F. Eck (2010), Global evaluation of the Collection 5 MODIS dark-target aerosol products over land, *Atmos. Chem. Phys.*, *10*, 10,399–10,420.
- Li, Z., F. Niu, J. Fan, Y. Liu, D. Rosenfeld, and Y. Ding (2011), Long-term impacts of aerosols on the vertical development of clouds and precipitation, *Nat. Geosci.*, *4*(12), 888–894.
- Loeb, N. G., and G. L. Schuster (2008), An observational study of the relationship between cloud, aerosol and meteorology in broken low-level cloud conditions, *J. Geophys. Res.*, *113*, D14214, doi:10.1029/2007JD009763.
- Long, C. N., J. M. SABBURG, J. Calbo, and D. Pages (2006), Retrieving cloud characteristics from ground-based daytime color all-sky images, *J. Atmos. Oceanic Technol.*, *23*(5), 633–652.
- Mauger, G. S., and J. R. Norris (2007), Meteorological bias in satellite estimates of aerosol-cloud relationships, *Geophys. Res. Lett.*, *34*, L07815, doi:10.1029/2008GL033386.
- Myhre, G., F. Stordal, M. Johnsrud, Y. J. Kaufman, D. Rosenfeld, T. Storelvmo, J. E. Kristjansson, T. K. Berntsen, A. Myhre, and I. S. A. Isaksen (2007), Aerosol-cloud interaction inferred from MODIS satellite data and global aerosol models, *Atmos. Chem. Phys.*, *7*(12), 3081–3101.
- Nemesure, S., R. Wagener, and S. E. Schwartz (1995), Direct shortwave forcing of climate by the anthropogenic sulfate aerosol: Sensitivity to particle size, composition, and relative humidity, *J. Geophys. Res.*, *100*(D12), 26,105–26,116, doi:10.1029/95JD02897.
- Niu, F., and Z. Li (2012), Systematic variations of cloud top temperature and precipitation rate with aerosols over the global tropics, *Atmos. Chem. Phys.*, *12*, 8491–8498.
- Platnick, S., M. D. King, S. A. Ackerman, W. P. Menzel, B. A. Baum, J. C. Riedi, and R. A. Frey (2003), The MODIS cloud products: Algorithms and examples from Terra, *IEEE Trans. Geosci. Remote Sens.*, *41*(2), 459–473.
- Quaas, J., et al. (2009), Aerosol indirect effects—General circulation model intercomparison and evaluation with satellite data, *Atmos. Chem. Phys.*, *9*(22), 8697–8717.
- Quaas, J., B. Stevens, P. Stier, and U. Lohmann (2010), Interpreting the cloud cover—Aerosol optical depth relationship found in satellite data using a general circulation model, *Atmos. Chem. Phys.*, *10*(13), 6129–6135.
- Remer, L. A., et al. (2005), The MODIS aerosol algorithm, products, and validation, *J. Atmos. Sci.*, *62*(4), 947–973.
- Small, J. D., J. H. Jiang, H. Su, and C. Zhai (2011), Relationship between aerosol and cloud fraction over Australia, *Geophys. Res. Lett.*, *38*, L23802, doi:10.1029/2011GL049404.
- Stocker, T. F., D. Qin, G.-K. Plattner, M. Tignor, S. K. Allen, J. Boschung, A. Nauels, Y. Xia, V. Bex, and P. M. Midgley (2013), *IPCC: Climate Change 2013: The Physical Science Basis. Contribution of Working Group I to the Fifth Assessment Report of the Intergovernmental Panel on Climate Change*, Cambridge Univ. Press, Cambridge, U. K., and New York.

- Ten Hoeve, J. E., L. A. Remer, and M. Z. Jacobson (2011), Microphysical and radiative effects of aerosols on warm clouds during the Amazon biomass burning season as observed by MODIS: Impacts of water vapor and land cover, *Atmos. Chem. Phys.*, *11*(7), 3021–3036.
- Ten Hoeve, J. E., M. Z. Jacobson, and L. A. Remer (2012), Comparing results from a physical model with satellite and in situ observations to determine whether biomass burning aerosols over the Amazon brighten or burn off clouds, *J. Geophys. Res.*, *117*, D08203, doi:10.1029/2011JD016856.
- Torres, O., A. Tanskanen, B. Veihelmann, C. Ahn, R. Braak, P. K. Bhartia, P. Veefkind, and P. Levelt (2007), Aerosols and surface UV products from Ozone Monitoring Instrument observations: An overview, *J. Geophys. Res.*, *112*, D24547, doi:10.1029/2007JD008809.
- Twohy, C. H., J. A. Coakley Jr., and W. R. Tahnk (2009), Effect of changes in relative humidity on aerosol scattering near clouds, *J. Geophys. Res.*, *114*, D05205, doi:10.1029/2008JD010991.
- Varnai, T., and A. Marshak (2009), MODIS observations of enhanced clear sky reflectance near clouds, *Geophys. Res. Lett.*, *36*, L06807, doi:10.1029/2008GL037089.
- Yan, H., Z. Li, J. Huang, M. Cribb, and J. Liu (2014), Long-term aerosol-mediated changes in cloud radiative forcing of deep clouds at the top and bottom of the atmosphere over the Southern Great Plains, *Atmos. Chem. Phys.*, *14*, 7113–7124.
- Yuan, T., L. A. Remer, and H. Yu (2011), Microphysical, macrophysical and radiative signatures of volcanic aerosols in trade wind cumulus observed by the A-Train, *Atmos. Chem. Phys.*, *11*(14), 7119–7132.
- Zhao, C., S. A. Klein, S. Xie, X. Liu, J. S. Boyle, and Y. Zhang (2012), Aerosol first indirect effects on non-precipitating low-level liquid cloud properties as simulated by CAM5 at ARM sites, *Geophys. Res. Lett.*, *39*, L08806, doi:10.1029/2012GL051213.
- Zhou, M. (2006), *Advancing Assessments on Aerosol Radiative Effect by Measurement-Based Direct Effect Estimation and Through Developing an Explicit Climatological Convective Boundary Layer Model*, Ga. Inst. Technol.